

## RHEOLOGICAL AND FLOW MODELLING OF VISCOELASTIC FLUIDS BETWEEN ECCENTRIC CYLINDERS

Dana GRECOV and Kai LIU

Department of Mechanical Engineering, University of British Columbia, Vancouver, V6ZT 1Z4 CANADA

### ABSTRACT

Viscoelastic fluid flows within eccentric rotating cylinders are simulated using a commercial software finite element based, POLYFLOW, and an original approach based on stream-tube method (STM) and domain decomposition. The lubricant is modelled using an Upper Convective Maxwell (UCM) model. The results point out the influence of non-Newtonian properties of the fluids on annular flows between eccentric cylinders as also in particular cases of journal bearings, notably the role of elasticity. Significant viscoelastic effects are presented for all eccentric cylinders configurations.

### NOMENCLATURE

$\Omega$	inner cylinder angular velocity
$R_i$	radius of inner cylinder
$R_o$	radius of outer cylinder
L	axial length
e	eccentricity
$\mathbf{v}$	velocity vector
$\rho$	density
$p$	pressure
$\boldsymbol{\tau}$	stress tensor
$\dot{\gamma}$	shear rate,
$\dot{\gamma}_{ij}$	components of the rate of deformation tensor
$\mu$	viscosity
$\mu_0$	zero shear viscosity
$\mu_\infty$	viscosity at high shear rates
$\lambda$	relaxation time
n	material parameter.
$\nabla$	
$\boldsymbol{\tau}$	upper-convected time derivative of stress tensor
$\xi$	PTT parameter
$\varepsilon_l$	elongation parameter
$\varepsilon$	relative eccentricity
$V_c$	characteristic velocity
We	Weissenberg number
c	radial clearance
$C_f$	friction coefficient
$N_1$	first normal stress difference
$F_f$	friction force
$F_l$	load capacity

### INTRODUCTION

In this study, viscoelastic flows between eccentrically rotating cylinders are computed by using a commercial software POLYFLOW, based on finite element method and by the means of the stream-tube method (STM) (Grecov and Clermont, 2002, 2005) connected to journal bearing lubrication. The addition of polymers to Newtonian oils for industrial purposes has resulted in shear thinning and changes in elastic properties of the materials, thus leading to complex behavior in such eccentric rotating geometries. In the literature, numerous studies have been devoted to problems occurring in eccentric rotating cylinders with various methods for computing the flow characteristics. The viscoelastic fluid effect on eccentric rotating cylinders is a long-standing and attractive subject in tribology.

For example, (Davies and Li, 1994) adopted a pseudo-spectral method with bipolar transformation to simulate nonisothermal flows between eccentrically rotating cylinders, using a White–Metzner viscoelastic differential model for the fluid. Beris et al., 1987 have studied steady flows between slightly eccentric cylinders, for inelastic and viscoelastic differential fluids, using a Galerkin finite-element method and a spectral finite-element technique. Similarly, the analysis proposed in (Chawda et al., 1996) involved numerical pseudospectral methods to compute steady-state flow between eccentric rotating cylinders and to explore the stability of three dimensional disturbances, for an upper-convected Maxwell fluid. In order to investigate specific lubrication problems related to the separate and combined effects of shear thinning, temperature thinning and temperature thickening in two-dimensional journal bearings, a recent study involving spectral elements has been proposed in (Li et al., 2000)

Furthermore, a study by X.Huang et al. (Huang et al., 1996) investigated UCM fluids within eccentric rotating cylinders at low eccentricities in steady state (inertia neglected). In (Berker et al., 1995) and (Williamson et al., 1997) it was experimentally assessed the effect of polymer additives in journal bearings for several multi-grade lubricants and

found that viscoelasticity of the multigrade oils did indeed produce a measurable and beneficial effect on lubrication characteristics such as load capacity at high eccentricity ratios.

Using a combined spectral element method with an ALE formulation, (Gwynllyw and Phillips, 2008) assessed the influence of the relaxation time for Oldroyd-B and PTT fluids on the load bearing characteristics. Dynamic journal bearings were investigated for Cross fluids (Li et al., 2000) and couple stress fluids (Chang-Jian, 2007).

However, the effect of fluid viscoelasticity on the flow between eccentric rotating cylinders is not yet completely elucidated. The main challenge is to obtain the numerical convergence for high

viscoelastic fluids in narrow and moderate gap for a three dimensional time dependent problem. The ultimately objective of this study is to reveal the viscoelastic effects on flows between eccentric rotating cylinders and on the lubrication performances.

#### MODEL DESCRIPTION

One of the main objectives of this paper is to apply analyses based on stream-tube methods (Grecov and Clermont, 2002, 2005) (Grecov et al., 2002) that may enable flows of incompressible fluids obeying viscoelastic constitutive equations to be simulated using simple computational domains. Calculations, corresponding here to steady and isothermal situations, are related to a stream tube method that provides possibilities to compute main flow zones as well as vortex regions using domain decomposition and local transformation functions. The analysis permits accurate calculations of annular flows for various constitutive equations, with spatial variables in a simple computational domain. An extended description of the method is presented in previous papers (Grecov and Clermont, 2002, 2005) for steady state calculations for high viscoelastic flows. However, in recent paper (Clermont and Grecov, 2009) developed a new formulation for unsteady calculations.

The viscoelastic flows between eccentric cylinders are also calculated using POLYFLOW. The different numerical method used by this software allows calculating 2 D and 3 D transient flows, for moderate viscoelasticity.

The inner cylinder of radius  $R_1$  rotates with an angular velocity  $\omega$ . The outer cylinder of radius  $R_0$ , is at rest. The parameter  $e$  denotes the distance between the axes of the cylinders. The eccentricity is defined as  $\varepsilon=e/(R_0 - R_1)$ . Figure 1 presents the schematic of eccentric annulus geometry. A Cartesian system of coordinates is used and the centre of outer cylinder is set as the origin.

The governing equations for the annulus flows are presented as follows:

$$\nabla \cdot \mathbf{V} = 0 \quad (1)$$

$$\rho \left( \frac{\partial \mathbf{V}}{\partial t} + \mathbf{V} \cdot \nabla \mathbf{V} \right) = -\nabla p + \nabla \cdot \boldsymbol{\tau} + \rho \mathbf{g} \quad (2)$$

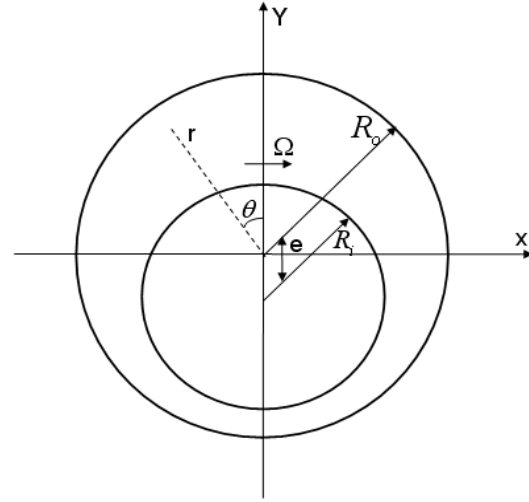


Figure 1: Schematic of the eccentric annuli geometry.

#### Constitutive equations

For generalized Newtonian constitutive models, the relationship between the stress tensor and rate of the deformation tensor is as follows.

$$\boldsymbol{\tau} = \mu(\dot{\gamma}) \cdot \dot{\boldsymbol{\gamma}} \quad (3)$$

Carreau fluid viscosity function (Macosko, 1994) is given by:

$$\frac{\mu - \mu_0}{\mu_0 - \mu_\infty} = [1 + (\lambda \dot{\gamma})^2]^{n-1/2} \quad (4)$$

Viscoelastic constitutive models include memory effects caused by elasticity of material. The stress tensor is a function of the history of rate of deformation tensor instead of a function of instantaneous rate of deformation tensor. Two viscoelastic models - Upper Convected Maxwell (UCM) model and Phan-Thien-Tanner (PTT) model are considered in this work.

UCM model is a differential generalization of Maxwell model for the case of large deformations based on the upper-convected time derivative. The model can be written as (Macosko, 1994)

$$\boldsymbol{\tau} + \lambda \overset{\nabla}{\boldsymbol{\tau}} = \mu_0 \dot{\boldsymbol{\gamma}} \quad (5)$$

$\overset{\nabla}{\boldsymbol{\tau}}$  is upper-convected time derivative of stress tensor which is expressed as:

$$\overset{\nabla}{\boldsymbol{\tau}} = \frac{\partial}{\partial t} \boldsymbol{\tau} + \mathbf{V} \cdot \nabla \boldsymbol{\tau} - (\nabla \mathbf{V})^T \cdot \boldsymbol{\tau} - \boldsymbol{\tau} \cdot (\nabla \mathbf{V}) \quad (6)$$

The complete form of PTT constitutive equation is (Macosko, 1994):

$$f(tr_\tau) \cdot \boldsymbol{\tau} + \lambda \overset{\nabla}{\boldsymbol{\tau}} + \frac{\xi}{2} \lambda (\dot{\boldsymbol{\gamma}} \cdot \boldsymbol{\tau} + \boldsymbol{\tau} \cdot \dot{\boldsymbol{\gamma}}) = \mu \dot{\boldsymbol{\gamma}} \quad (7)$$

The linearized form of stress function is:

$$f(tr_\tau) = 1 + \frac{\varepsilon_1 \lambda}{\mu} tr_\tau \quad (8)$$

#### NUMERICAL PROCEDURE

For the stream tube method, the governing equations involve the dynamic and constitutive equations, together with boundary condition relations. Mass

conservation is automatically verified. We adopted a mixed formulation where the unknowns are the pressure, the mapping functions and the stress components (Grecov and Clermont, 2002). Owing to the rectangular mesh defined in the computational sub-domains, finite-difference formulae are adopted to approximate the derivatives involved in the equations and regular meshes were used to discretize the equations and unknowns in terms of the transformation functions and their derivatives (Grecov et al., 2002). The code, was implemented on a server (Sun Fire X4450  $\times$ 64 with 4  $\times$  Quad-core Intel Xeon X7350 processor and 16 GB memory). Tests were performed for inelastic (Newtonian and purely viscous Carreau) fluids and viscoelastic materials modelled by differential equations, for which comparisons with data from the literature were possible (Grecov and Clermont, 2005).

Numerical simulations of the mathematical model are performed using POLYFLOW software on the same server. POLYFLOW is finite-element computational fluid dynamics software designed primarily for viscoelastic fluid dynamics applications. Various domain meshing methods and numerical schemes are tested and compared to obtain effective and efficient numerical systems for 2D and 3D numerical simulations.

Figure 2 presents a 3D mesh for UCM fluids numerical simulations ( $R_o=6$  cm,  $R_i=5.084$  cm, axial length  $L=8$  cm, and  $\varepsilon=0.7$ ). Non-slip boundary conditions were imposed on both cylinders, and periodic boundary conditions (with zero normal force) were used at both axial ends. In numerical simulations, evolution methods for angular velocity of inner cylinder and EVSS (Elastic Viscous Split Stress) interpolation scheme for stress were used to reach numerical convergence.

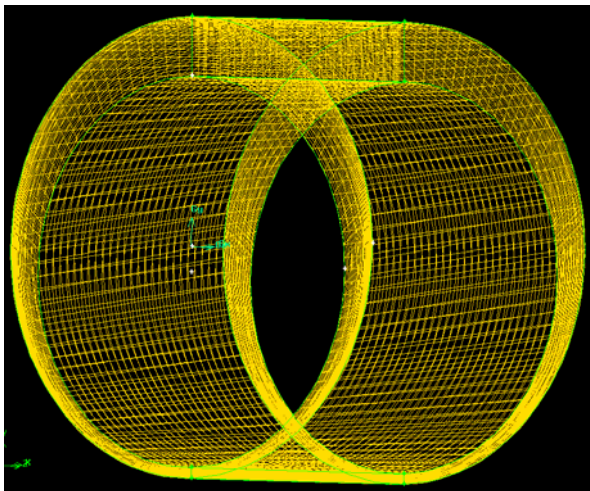


**Figure 2:** Finite element mesh for 3D UCM at eccentricity ratio  $\varepsilon=0.7$

Different validations based on analytical solutions, experiment results and other numerical simulations were performed.

As an example, figure 3 presents the computed wall shear stresses at low angular velocity which are in good agreement with analytical results developed in (Mirazadeh et al., 2005) for purely tangential flow of a SPTT fluid within a concentric annulus ( $R_i=5.084$  cm and  $R_o=6$  cm). There is an increasing deviation between the numerical results and analytical solutions as the angular velocity increases. This is caused by the assumptions used in the derivation of analytical solution - purely tangential flow and thin film theory.

Comparisons between the numerical results using STM and POLYFLOW were performed and found in good agreement.

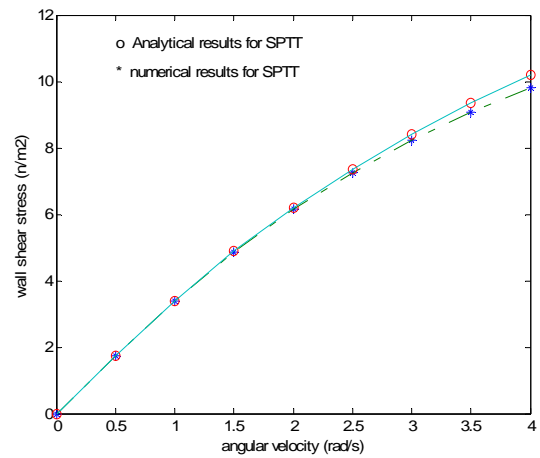


**Figure 3:** Wall shear stress at the inner rotating cylinder versus angular velocity in concentric annulus for a SPTT fluid. o- analytical solution; \*-numerical results – POLYFLOW.

#### 4. NUMERICAL SIMULATION RESULTS

The viscoelasticity is characterized by a dimensionless number, Weissenberg number, which is the ratio of the relaxation time of fluid and a specific process time. It is defined as  $We = \frac{\lambda V_c}{c}$ ,

where  $V_c$  is expressed as  $V_c = \frac{R_i + R_o}{2} \Omega$  and

$c = R_o - R_i$ . The inner cylinder is rotating steadily

clockwise at an angular velocity of 5.24 rad/s. Other parameters for UCM fluid properties and the geometry of eccentric cylinders are selected as follows:  $\mu=0.3$

Pa.s,  $\rho = 900 \text{ kg/m}^3$ ,  $R_o=6$  cm,  $R_i=5.084$  cm, and  $\varepsilon = 0.7$ .

#### Two dimensional flows

##### POLYFLOW results

In this paragraph, we present results obtained using POLYFLOW, for a 2D flow domain (figure 1) with low viscoelasticity (maximum  $We=5$ , limited by POLYFLOW capabilities).

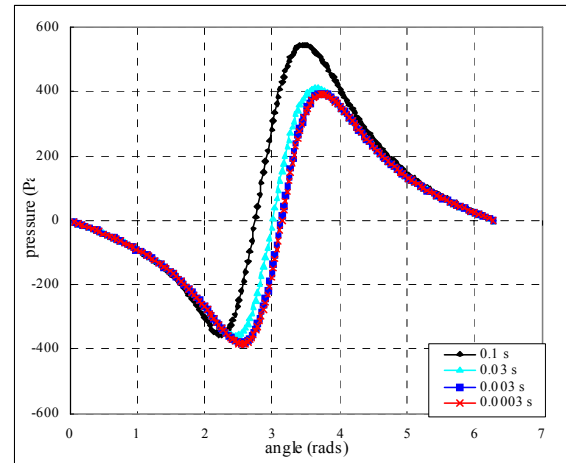
In order to evaluate the viscoelastic effects of UCM fluid on the flow, various relaxation times varying from 0.0003 s to 0.1 s for UCM fluids are studied corresponding to a maximum of  $We=3.5$ .

Figure 4 presents the pressure profiles along the inner cylinder for various relaxation times. The profiles shift to left with the increase of relaxation time. This effect of relaxation time on pressure is very important for journal bearing performance, as the pressure around the inner cylinder is the main factor to generate load capacity in a journal bearing. When the relaxation time is small such as lower than 0.003 s, the pressure profile is close to anti-symmetric pressure profile for a Newtonian fluid. For the relaxation time of 0.1 s, the pressure profile clearly shifts to the left and deviates from anti-symmetry strongly. The difference between extreme high and low pressures increases with relaxation time.

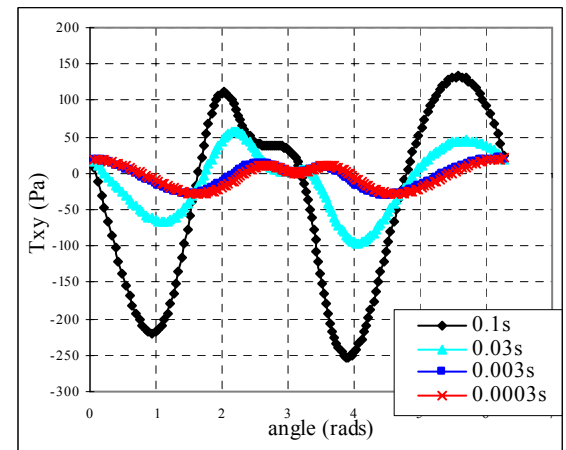
Figure 5 presents the profiles of shear stress along the inner cylinder for various relaxation times. The profile of shear stress for a low relaxation time of 0.0003 s is very close to the symmetric shear stress profile for a Newtonian fluid. While the relaxation time further increases, the shape of shear stress profile changes essentially. For the relaxation time of 0.1 s, the lowest shear stress in the range of 3-4 radians decreases greatly, while the increase of the highest shear stress in the range of 2-3 radians is relatively low, comparing with the shear stress profile for the relaxation time of 0.03 s. The variation of shear stress profile with relaxation time evidently reveals the viscoelastic effects, which can affect both the load capacity and moment on the journal for journal bearing applications.

Figure 6 presents the profiles of normal stress differences ( $N_1 = \tau_{xx} - \tau_{yy}$ ) along inner cylinder for various relaxation times. For low relaxation times, the normal stress difference profiles are almost flat. For high relaxation time the highest value of normal stress difference reaches 500 Pa which is 2.5 times the highest value at the relaxation time of 0.03 s and nearly 10 times the highest value for the relaxation time of 0.003 s. The first normal stress difference profiles show an important viscoelastic effect at a relatively high relaxation time.

Figure 7 presents the evolution of load capacity on the inner cylinder for various relaxation times of UCM fluid. When the relaxation time is as low as 0.0003 s, the evolution of load capacity on the journal gradually increases until the steady state is reached. As the relaxation time increases, there is a slight fluctuation characteristic in the evolution of load capacity. For higher relaxation time of 0.1 s, the scale and number of fluctuations are much greater, and it takes much more time to reach the steady state of flow, pointing out the dominant influence of elastic properties with respect to viscosity effects.



**Figure 4:** Pressures along the inner cylinder for the UCM fluids of various relaxation times ( $\lambda=0.0003$  s-0.1 s).



**Figure 5:** Shear stresses along the inner cylinder for the UCM fluids of various relaxation times ( $\lambda=0.0003$  s-0.1 s).

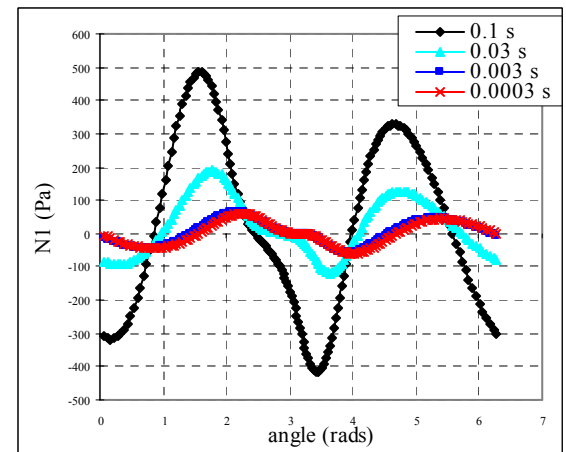


**Figure 6:** First normal stress differences along the inner cylinder for the UCM fluids of various relaxation times ( $\lambda=0.0003$  s-0.1 s).

Figure 8 presents the variation of load capacity with Weissenberg number for Newtonian and UCM fluids. When the relaxation time of UCM fluid is

lower than 0.03 s, the load capacity for Newtonian ( $\mu=0.3 \text{ Pa}\cdot\text{s}$ ,  $\rho=900 \text{ kg}/\text{m}^3$ ) and UCM fluids are very close.

With further increase of Weissenberg number (through increasing relaxation time), the load capacity on the inner cylinder gradually increases. The gradient of load capacity increases with Weissenberg number.

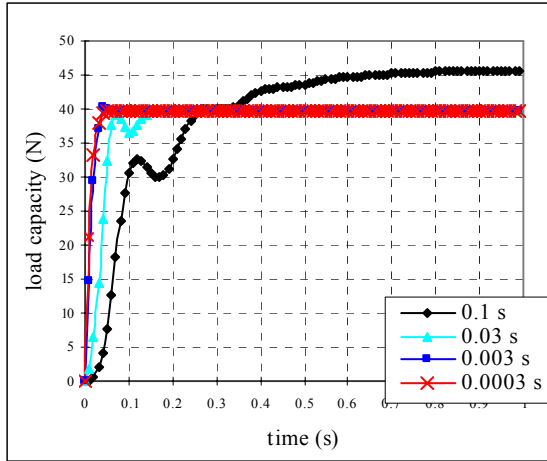


**Figure 7:** Transient load capacity on the inner cylinder in start-up flow for the UCM fluids of various relaxation times ( $\lambda=0.0003 \text{ s} - 0.1 \text{ s}$ ).

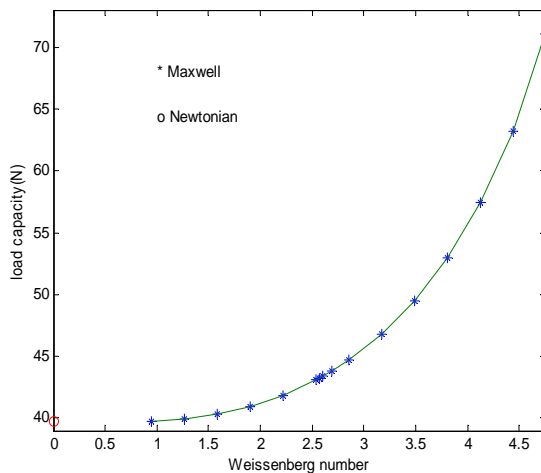


**Figure 8:** Load capacity on the inner cylinder versus Weissenberg number for Newtonian and UCM fluids.

It indicates that the load capacity can be greatly improved by increasing the relaxation time of UCM fluid. Higher load capacity can be achieved using UCM fluids rather than Newtonian fluids. This is a beneficial effect of viscoelasticity on journal bearing performance. High load capacity greatly decreases the contact opportunity between two relatively moving surfaces and make journal bearings work more efficiently and safely.

Friction in journal bearings is characterized by a dimensionless number, friction coefficient, which is calculated from:  $C_f = \frac{F_f}{F_l}$ .

Figure 9 presents the friction coefficient versus Weissenberg number for Newtonian and UCM fluids. It can be found that the friction coefficient increases with Weissenberg number. This is a by-side effect for lubrication performance using UCM fluids comparing with the Newtonian fluid. For low Weissenberg numbers, the friction coefficient increases greatly, but the gradient of friction coefficient with Weissenberg number decreases for Weissenberg numbers between 1 and 3.5, and a nearly plateau region is reached for Weissenberg numbers in the range of 2.5– 3.5.

In our numerical simulations the maximum Weissenberg number is 5, limited by POLYFLOW capabilities.

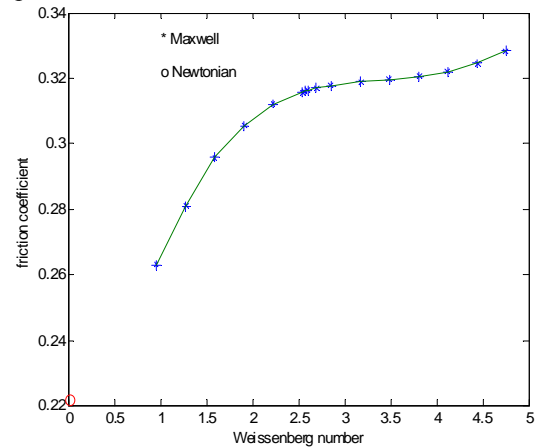


**Figure 9:** Friction coefficient versus Weissenberg number for Newtonian and UCM fluids.

#### Stream-tube method results

We present here results for a 2D geometry, with UCM fluid, for high viscoelasticity using the stream tube method based code. The limit of convergence with a UCM fluid was found to correspond to a Weissenberg number around 80.

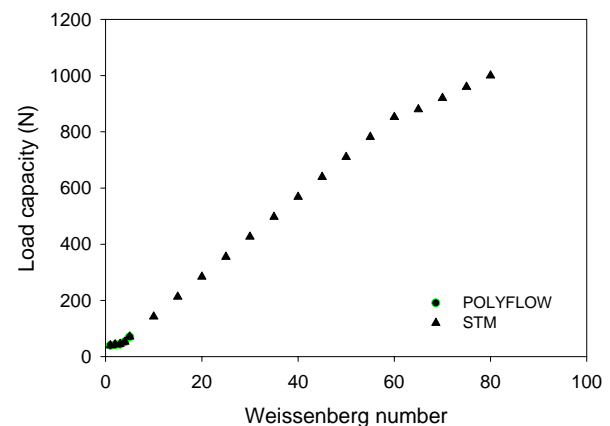


**Figure 10:** Load capacity on the inner cylinder versus Weissenberg number for UCM fluid (POLYFLOW and STM results).

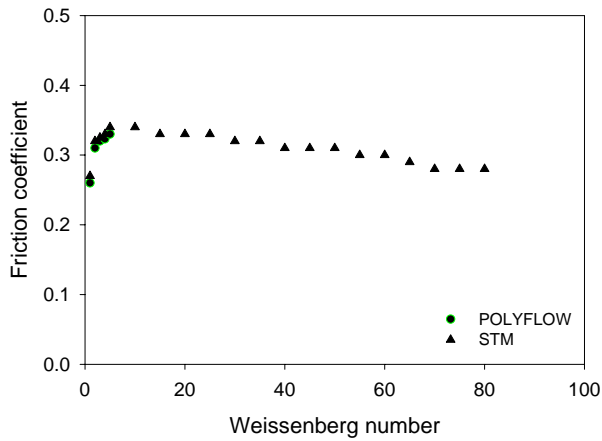


**Figure 11:** Friction coefficient versus Weissenberg number for UCM (POLYFLOW and STM results).

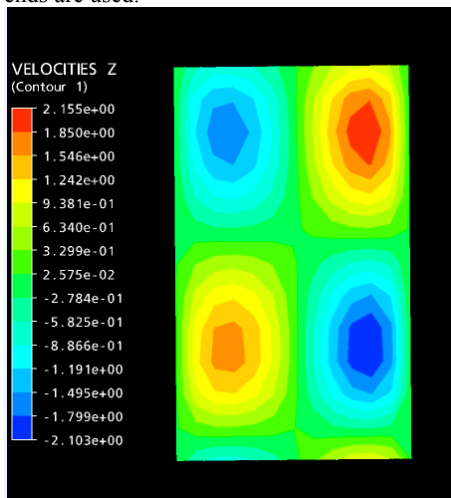
Figure 10 presents the load capacity on the inner cylinder versus Weissenberg number for UCM fluid, using POLYFLOW and Stream tube method based code. It shows that the load capacity can be greatly improved by increasing the viscoelasticity (We number) of UCM fluid.

Figure 11 presents the friction coefficient versus Weissenberg number for UCM fluid, based on results using POLYFLOW and STM based code. It shows that the at relatively high We numbers the friction decreases, so the lubrication performances for highly viscoelastic fluids are improved.

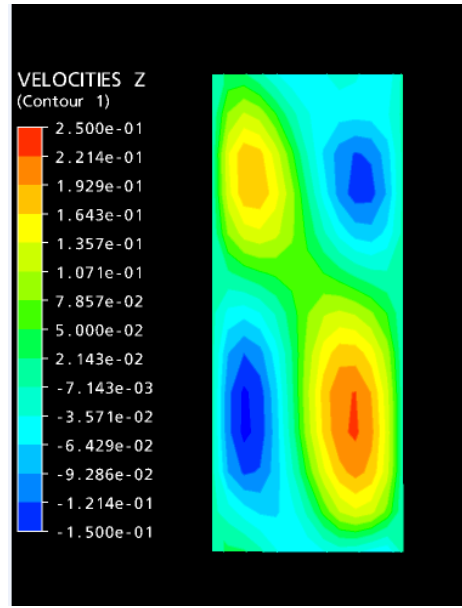
### Three dimensional flows

Steady state flow for Newtonian and UCM fluids within eccentric rotating cylinders are investigated in 3D numerical simulations using POLYFLOW.

In this simulation, Taylor vortex flow within eccentric rotating cylinders is presented. The fluid is Newtonian ( $\mu=0.099$  Pa.s and  $\rho=1048\text{kg}/\text{m}^3$ ) and periodic boundary conditions (with zero normal force) at both axial ends are used.



a)

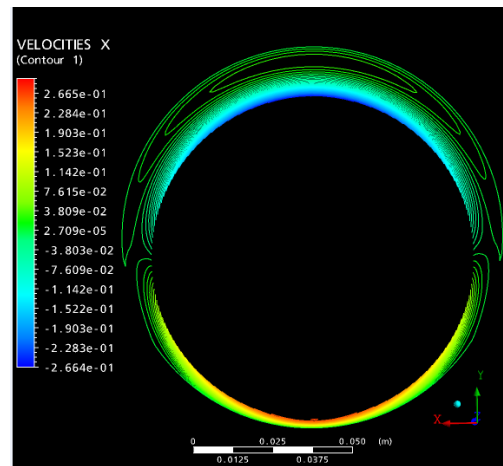


b)

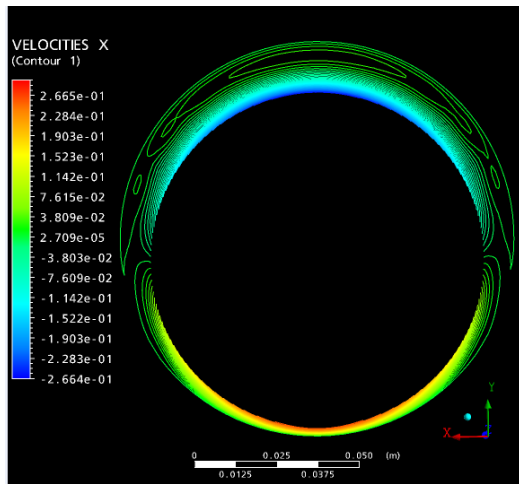
**Figure 12:** Z-velocity contours ( $\Omega=6500$  rad/s) for the Newtonian fluid at YZ cross-section ( $X=0$ ) in the widest gap (a) and in the narrowest gap (b).

The 3D geometry is created as follows:  $R_o=2.54$  cm,  $R_i=2.5146$  cm, length  $L=0.0508$  cm, and  $\varepsilon=0.2$ .

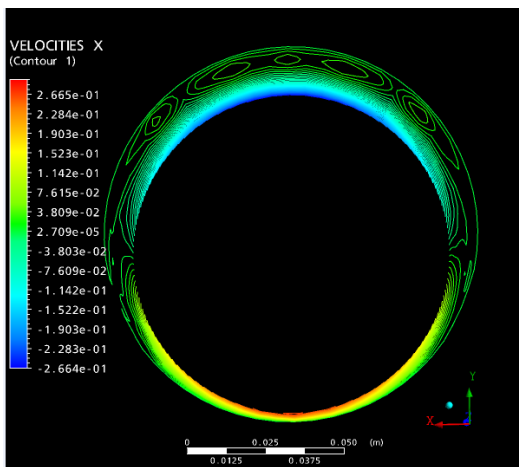
The angular velocity of inner cylinder is 6500 rad/s. Figure 12 presents Z-velocity contours at YZ cross-section ( $X=0$ ) for the widest and narrowest gaps respectively. The Taylor vortex flow is clearly observed in this eccentric annuli flow.



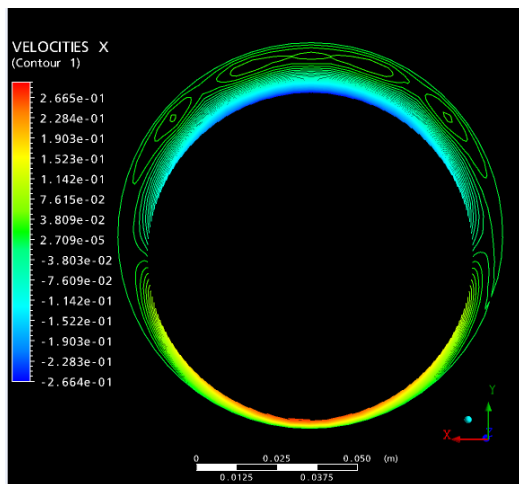
a)



b)



c)



d)

**Figure 13:** X-velocity contours ( $\Omega=5.24$  rad/s) for UCM fluid ( $\lambda=0.03$  s) in XY cross-sections at different axial positions a)  $z=4$  cm ; b)  $z=7.3$  cm, c)  $z=7.5$  cm, d)  $z=7.7$  cm .

The UCM fluid with  $\mu =0.3$  Pa.s,  $\rho =900$  kg /m<sup>3</sup>,  $\lambda =0.03$  s, is used for the 3D

study. The inner cylinder is rotating at an angular velocity of 5.24 rad/s.

Figure 13 presents X-velocity contours for the UCM fluid in XY cross-sections at different axial positions. In the wide gap, from the axial middle position ( $z=4$  cm) to the end ( $z=7.3$  cm,  $z=7.5$  cm and  $z=7.7$  cm), the recirculation size decreases and the break of recirculation contours could be observed.

## CONCLUSION

Numerical simulations for viscoelastic fluids flow within eccentric rotating cylinders are performed using commercial finite element software POLYFLOW and an original approach using a stream-tube method and domain decomposition. POLYFLOW enables calculation for moderate viscoelasticity, though 3 D and transient. STM method enables 2D calculations for steady state, though for high viscoelasticity, due to the efficiency and robustness of this method. Overall, numerical results revealed that lubrication performances are greatly affected by the viscoelasticity of fluid. Increased load capacity on the inner cylinder can be achieved by increasing viscoelasticity of flow. The friction increased for low Weissenberg numbers (viscoelasticity) and started to have an important decrease for high Weissenberg numbers, leading to an improvement on lubrication performances.

## ACKNOWLEDGMENTS

The financial support from the Natural Sciences and Engineering Research Council (NSERC) of Canada is gratefully acknowledged. The computational resource funded by the Canada Foundation for Innovation (CFI) is also acknowledged.

## REFERENCES

- BERIS A.N., ARMSTRONG R.C. and BROWN R.A.,(1987), "Spectral/finite element calculations of the flow of a Maxwell fluid between eccentric rotating cylinders", *J. Non-Newtonian Fluid Mech.*, **22**,129–167.
- BERKER A., BOULDIN M.G.,KLEIS S.J and VANARSDALE ,W.E., (1995), "Effect of polymer on flow in journal bearing", *J. Non-Newtonian Fluid Mech.*,**56**, 333-347.
- CHANG-JIAN CW., (2007), " Nonlinear dynamic response of couple stress fluid film bearing system with nonlinear suspension and roughness effect", *J. of the Chinese Society of Mechanical Engineers*, **28** (4), 375-384.
- CHAWDA A. and AVGOUSTI M., (1996), "Stability of viscoelastic flow between eccentric rotating cylinders", *J. Non-Newtonian Fluid Mech.*, **63**, 97–112.
- CLERMONT, J.R. and GRECOV D., (2009), "A theoretical analysis of unsteady incompressible flows for time-dependent constitutive equations based on domain transformations", *I. Journal of Non-Linear Mech.*, **44**, 709-715.
- DAVIES A.R. and LI X.K., (1994), "Numerical modeling of pressure and temperature effects in viscoelastic flow between eccentrically rotating cylinders", *J. Non-Newtonian Fluid Mech.* **54**, 331–350.

GRECOV D. and CLERMONT J.R., (2002), "Numerical study of flows of complex fluids between eccentric cylinders using transformation functions", *Int. J. Numer. Methods Fluids*, **40** (5), 669–696.

GRECOV D., CLERMONT, J.-R. , and NORMANDIN M., (2002), "A numerical approach for computing flows by local transformations and domain decomposition using an optimization algorithm", *Comput. Methods Appl. Mech. Eng.*, **191** (39–40), 4401–4419.

GRECOV D. and CLERMONT J.R., (2005), "Numerical simulations of non-Newtonian flows between eccentric cylinders by domain decomposition and stream-tube method", *J. Non-Newtonian Fluid Mech.*, **126**, 175-185.

GWYNLLYW D. and PHILLIPS T.N, (2008), " The influence of Oldroyd-B and PTT lubricants on moving journal bearing systems", *J. Non-Newtonian Fluid Mech.*, **150**, 196-210.

HUANG X., PHAN-THIEN N and TANNER R., (1996), "Viscoelastic flow between eccentric rotating cylinders: Unstructured control volume method", *J. Non-Newtonian Fluid Mech.*, **64**, 71-92.

LI X.K., GWYNLLYW D., DAVIES A.R. and PHILLIPS T.N, (2000), " On the influence of lubricant properties on the dynamics of two-dimensional journal bearings", *J. Non-Newtonian Fluid Mech.*, **93**, 29–59.

MACOSKO C.W., (1994), "Rheology: principles, measurements and applications", Wiley-VCH, New York

MIRAZADEH M. and ESCUDIER M.P, (2005), "Purely tangential flow of a PTT-viscoelastic fluid within a concentric annulus", *J. of Non-Newtonian Fluid Mechanics*, **129**, 88-97.

WILIAMSON B.P., WALTERS K, BATES T.W., COY R.C and MILTON A.L., (1997), "The viscoelastic properties of multigrade oils and their effect on journal-bearing characteristics", *J. Non-Newtonian Fluid Mech.*, **73**, 115-126.